PROCEEDINGS OF THE THIRD INTERNATIONAL CONFERENCE ON
HYDROINFORMATICS/COPENHAGEN/DENMARK/24-26 AUGUST 1998

HYDROINFORMATICS '98

Edited by

Vladan Babovic & Lars Christian Larsen
Danish Hydraulic Institute, Hørsholm, Denmark

OFFPRINT

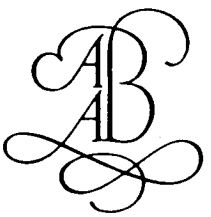

A.A.BALKEMA/ROTTERDAM/BROOKFIELD/1998

Hydroinformatics'98, Babovic & Larsen (eds) © 1998 Balkema, Rotterdam, ISBN 90 5410 983 1

GRId-based variable source area STOrm Runoff Model (GRISTORM)

S.J. Kim
Konkuk University, Seoul, South Korea
T.S. Steenhuis
Cornell University, Ithaca, N.Y., USA

ABSTRACT: A GRId-based STOrm Runoff Model (GRISTORM) which predicts temporal variations and spatial distributions of subsurface flow and saturated overland flow with in a watershed shallow soil depths in a watershed was developed. This model uses ASCII-formatted map data supported by the regular gridded map of the GRASS Geographic Information System (GIS) and generates the temporal and spatial distribution of discharge, flow depth and soil moisture in overland flow areas.

INTRODUCTION

Understanding of nonpoint source pollutants is becoming increasingly important in establishing environmental protection plans for watersheds. It is necessary to find a way to predict temporal/spatial distribution and transport patterns of pollutants. During a hydrologic year, storm events are an important factor in pollutant transport. A hydrologic model which predicts surface and subsurface flows and their flowpaths to the stream is required.

Recently, several researchers have attempted to model the rainfall-runoff process with Geographic Information System. GIS has proven to be an efficient tool for spatial analyses and visualizing the results of hydrologic and water quality modeling.

The source area for overland flow in a watershed shrinks and expands in response to rainfall (Tischendorf, 1969). The source area may be regarded as an expansion of the perennial channel system into zones of low storage capacity fed from below by subsurface stormflow and by rainfall from above. During rainless periods, streams are fed, to a large extent, by moisture migrating slowly downslope under conditions of unsaturated flow (Kirkby, 1978). As Dunne and Black (1970) point out, the source area generates overland flow, whereas the remainder of the watershed acts mainly as a reservoir during storms to provide baseflow after the storm and to maintain the wet areas that will produce subsequent storm runoff. A GIS can help to apportion storm runoff between the various flow sources associated with source areas on slopes.

Allen (1987) developed SWHAM (Small Watershed Hydrologic Analysis Model) using a GIS. The model is an overland flow model which is composed of a one-dimensional groundwater hydrologic model, stream flow model and digital map. Input data were extracted from soil, land use/cover and contour map. Stuebe and Johnston (1990) applied GIS to all phases of the SCS (Soil Conservation Service) modeling processes, including watershed delineation and routing of runoff to estimate the outlet runoff volume. Stuebe and Johnson's work demonstrated the use of GRASS to estimate runoff via the SCS Runoff Curve Number Model. Famiglietti (1992) used grid data extracted from a GIS and developed a GIS model using grid-based water balance and flow equation. Zollweg (1994) developed SMoRMod (Soil Moisture-based Runoff Model) using a series of GRASS commands. The model is a grid-based rainfall-runoff model which is composed of a daily soil moisture balance and sub-routines which calculate runoff generation/transport at 30-minute intervals. The initial conditions for the runoff generation are provided by the daily soil moisture balance. The model has a tendency to either over- or under-predict the recession part of hydrographs. Savabi et al. (1995) used GRASS to obtain WEPP (Water Erosion Prediction Project) model's input parameters. Frankenberger (1996) modified

Zollweg's GIS-Based Variable Source Area Model using GRASS. The model, written in UNIX-shell script, predicts daily soil moisture and runoff based on a water balance for shallow soils.

In this paper, a grid-based subsurface and saturated overland/stream flow generation procedure is described. This approach predicts the temporal variation and spatial distribution of overland flow depth, discharge and soil moisture during a storm event. The procedure's applicability and its modification of the surface and subsurface kinematic modeling approach (Takasao and Shiiba, 1988) are described. The model runs on the GRASS and uses regular gridded data such as elevation, stream, land use and soil information. The data were previously developed and described in Frankenberger's Ph.D. thesis (1996). A storm runoff model coded in UNIX-C uses this information and displays the results on GRASS.

2. MODEL DESCRIPTION

2.1 Saturated overland/stream flow and subsurface flow model

Storm runoff in the northeastern United States originates mainly from the saturated areas (Dunne and Black, 1970). Saturated areas often form where lateral subsurface flows converge, slopes change, or where depth to the restricting layer decreases (Frankenberger, 1996). The amount of runoff is directly related to the magnitude of the saturated areas.

In order to model the formation of variable source areas, we adopted the combined surface-subsurface kinematic modeling approach (Takasao and Shiiba, 1988). The continuity equation applied to each grid element can be written as in Equation 2.1. The schematic representation of the flow system is shown in Figure 1.

$$\frac{\partial A}{\partial t} + \frac{\partial Q}{\partial x} = \frac{r A_c}{L_c} + \frac{Q_\ell}{L_\ell} \qquad (2.1)$$

where A = flow area (m^2); Q = discharge (m^3/sec); r = rainfall intensity (m/sec); A_c = grid element area (m^2); L_c = flow distance through the grid element (m); Q_ℓ = lateral discharge (m^3/sec); L_ℓ = lateral flow length (m); t = time (sec); ℓ = length (m).

The flow areas for subsurface and saturation overland/stream flow are,

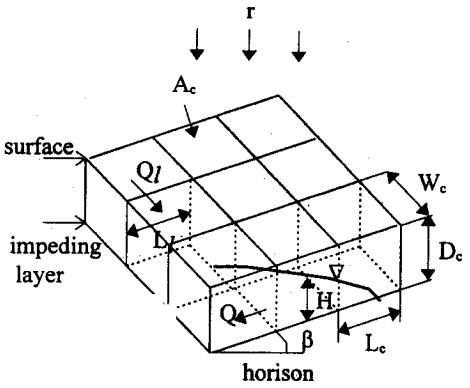

Figure 1 Schematic representation of the flow system.

$$A = W_c\ EP_c\ H, \qquad 0 \le H \le D_c \qquad (2.2)$$
$$= W_c\ EP_c\ D_c + A_f, \qquad H > D_c \qquad (2.3)$$

where W_c = grid element width orthogonal to streamline (m); EP_c = total porosity minus field capacity (m^3/m^3); D_c = soil depth above the impeding layer (m); H = flow depth above the impeding layer (m); A_f = overland flow area (= W_c (H-D_c)) (m^2).

The resistance equation for subsurface flow, and the kinematic wave equation for saturation overland/stream flow are obtained by the Darcy and Manning equations respectively:

$$Q = K_e\ A / EP_c\ \sin(\beta), \qquad 0 \le H \le D_c \qquad (2.4)$$
$$= W_c\ H\ K_e\ \sin(\beta)$$
$$= W_c\ D_c\ K_e\ \sin(\beta) + \alpha\ A_f^m \qquad H > D_c \qquad (2.5)$$

where K_e = unsaturated hydraulic conductivity (m/sec); β = grid element slope (degree), m= 5/3 for overland flow, 4/3 for stream flow; $\alpha = n^{-1}\ W_c^{-2/3}\ \tan^{1/2}\beta$ for overland flow, $n^{-1}\ \gamma^{2/3}\ \tan^{1/2}\beta$ for stream flow; n = Manning's roughness coefficient; $\gamma = R_h\ A_f^{-1/2}$ (Moore and Foster, 1990; Moore and Burch, 1986); R_h = hydraulic radius.

The finite difference form of Equation 2.1 is expressed as

$$A_4 + 2Q_4 \frac{Dt}{L_c} = A_1 - A_2 + A_3 + 2Q_2 \frac{Dt}{L_c} + 2rA_c \frac{Dt}{L_c} + 2Q_\ell \frac{Dt}{L_c}$$

where Δt = time interval; A_1, A_3 = flow area at time t at the inlet and outlet of the grid element respectively; A_2, A_4 = flow area at time $t + \Delta t$ at the inlet and outlet of the grid element respectively.

To solve Equation 2.6, Brakensiek's four-point implicit scheme (1967) was adopted. The equation was rearranged to solve for flow depth (H), and Newton-Raphson method was used to calculate it at the outlet of the grid element after a given time interval.

2.2 Initial and boundary flow depth conditions of various shallow soil depths

The spatial distribution of initial flow depths in a watershed can be obtained from soil information maps describing porosity, field capacity and initial soil moisture conditions. The initial flow depth for each grid element can be calculated by

$$\begin{aligned} H_i &= D_c\,(SM_i - F_c)/(TP_c - F_c), && F_c < SM_i < TP_c \\ &= D_c, && SM_i \geq TP_c \\ &= 0, && SM_i \leq F_c \end{aligned} \quad (2.7)$$

where H_i = initial flow depth in grid element (m); SM_i = initial soil moisture content in grid element (m^3/m^3); TP_c = total porosity in grid element (m^3/m^3); F_c = field capacity in grid element (m^3/m^3).

Since the data keep a constant value within each grid element, there exist two boundary values of flow depth between the neighboring grid elements. To remove a discontinuity in flow depth, a linear interpolation is used to obtain one flow depth on each grid element boundary.

In the case of changes in soil depth between grid elements, the boundary flow depth can be calculated as follows:

$$H_{i1}' = H_{i1} + [\,D_{c1} - H_{i1} - (D_{c2} - H_{i2})\,]/2, \quad H_{i1}' \geq D_{c1}-D_{c2} \quad (2.8)$$

$$= D_{c1} - D_{c2}, \quad H_{i1}' < D_{c1}-D_{c2} \quad (2.9)$$

$$H_{i2}' = H_{i1} - (D_{c2} - D_{c1}), \quad H_{i2}' \geq D_{c1}-D_{c2} \quad (2.10)$$

$$= 0, \quad H_{i2}' < 0 \quad (2.11)$$

where H_{i1}' = interpolated flow depth of the deep grid element, H_{i2}' = interpolated flow depth of the shallow grid element, H_{i1} = initial flow depth of the deep grid element, H_{i2} = initial flow depth of the shallow grid element, D_{c1} = deep soil depth element, D_{c2} = shallow soil depth element.

At the watershed boundary, flow depth conditions at the beginning side of the grid element are assumed zero.

2.3 Overland flow pattern and its classification

We can choose a 3 by 3 grid to determine flow direction. Firstly, the flow direction from the center grid element is determined by calculating slopes to the neighboring eight grid elements. Secondly, the subsurface/surface flow depth at the outlet of center grid is calculated by Equation 2.6 for a given time increment. Thirdly, the water of the grid element flows in the steepest direction. This means that a single output flowpath is chosen but the inflow to a grid element can come from multiple sources. If overland flows meet a stream, they are converted to lateral flow in the stream.

The flow condition in a grid element can be classified into four types. The first type is subsurface flow at both inlet and outlet of the grid element as follows:

$$\begin{aligned} &W_c EP_c H_4 + 2W_c H_4 K_c \sin\beta\, Dt/L_c \\ &= W_c EP_c (H_1 - H_2 + H_3) + 2W_c H_2 K_c \sin\beta\, Dt/L_c \\ &+ 2rA_c Dt/L_c + 2Q_\ell Dt/L_c \end{aligned}$$

where H_1, H_3 = flow depth at time t at the inlet and outlet of the grid element respectively; H_2, H_4 = flow depth at time $t + \Delta t$ at the inlet and outlet of the grid element respectively.

The second type is saturated overland flow, that is, surface flow conditions at both inlet and outlet as follows:

$$\begin{aligned} &W_c H_4 + 2\left[W_c (H_4 - D_c)\right]^m n^{-1} W_c^{-2/3} \tan^{-1/2}\beta\, Dt/L_c \\ &= W_c (H_1 - H_2 + H_3) + 2\left[W_c (H_2 - D_c)\right]^m n^{-1} W_c^{-2/3} \\ &\tan^{-1/2}\beta\, Dt/L_c + 2rA_c Dt/L_c + 2Q_\ell Dt/L_c \end{aligned}$$

The third type is a sink, that is, surface flow at the inlet and subsurface flow at the outlet. The last type is a source, that is, subsurface flow at the inlet and surface flow at the outlet. The last two cases cause a numerical divergence because of different flow conditions at the inlet and outlet of the grid element. Thus, in the third case, the flow depth at the inlet of grid element was assumed to be equal to soil depth D_c and solved by Equation 2.12. In the fourth case,

the starting point of surface flow within a grid element was linearly interpolated using the inlet flow depth H_1 and outlet grid depth H_3, and solved by Equation 2.13.

The stream flow is as follows:

$$W_c H_4 + 2\left[W_c (H_4 - D_c)\right]^{m+1/3} n^{-1} \left[W_c + 2(H_4 - D_c)\right]^{-2/3} \tan^{-1/2} b Dt / L_c = W_c (H_1 - H_2 + H_3) + 2\left[W_c (H_2 - D_c)\right]^{m+1/3} n^{-1} \left[W_c + 2(H_2 - D_c)\right]^{-2/3} \tan^{-1/2} b Dt / L_c + 2rA_c Dt / L_c + 2Q_\ell Dt / L_c \quad (2.14)$$

2.4 Model structure and implementation

A schematic flow diagram of the GRISTORM model is shown in Figure 2. As input data for the model, the seven GRASS regular gridded maps which are elevation, stream, land use, soil, porosity, field capacity and initial soil moisture condition are converted into ASCII-formatted map data using GRASS command r.out.ascii. The model uses this data to generate discharge, flow depth and soil moisture at each outlet of the grid element for a given time interval. In this study, the time step was 30 seconds. Stream flow at the watershed outlet and ASCII-formatted discharge maps, flow depth maps, and soil moisture maps were generated for 10-minute intervals. The ASCII-formatted map data were converted into GRASS maps using GRASS command r.in.ascii.

3. MODEL APPLICATION

3.1 Watershed, soils, land use and storm events

The model was tested on the Crowe Road watershed located in the Northern Catskill region of New York State. The watershed area is 170 ha and the elevation ranges from 580 m to 732 m.

The watershed soils are classified as inceptisols or entisols. The surface layer of most soils is shallow and permeable with a high percentage of rock fragments. Soil classifications and soil parameters that were verified by Frankenberger (1996) were used. Soil depths ranged from 28 cm to 150 cm and the percentage of rock fragments was between 10%

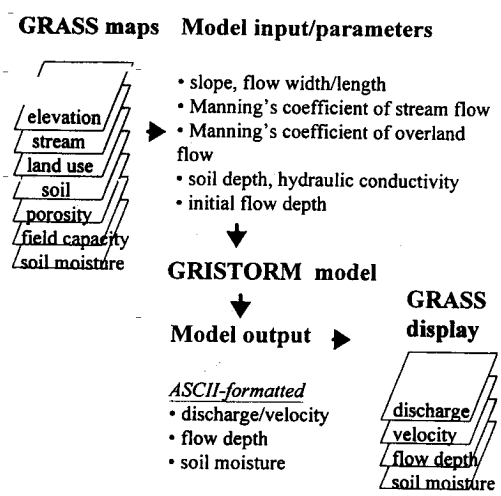

Figure 2. Schematic diagram of GRISTORM

and 40 %. The impeding layers are composed of bedrock, fragipan and clay. Saturated hydraulic conductivity in the surface layer is about 2 m/day. Average porosity and field capacity values without rocks are 0.6 and 0.37 respectively. Land use for the watershed was delineated by Frankenberger (1996).

Precipitation and stream flow data were measured at 10-minute intervals at the watershed outlet by the New York State Department of Environmental Conservation. Six storm events from July and August, 1994, were chosen for model calibration and verification.

3.2 Map data from GRASS

Seven maps containing information on elevation, stream, soil, land-use and soil parameters-porosity, field capacity and initial soil moisture condition-were used for input data. Elevation data were obtained from the USGS quadrangle vector map. Stream locations were obtained from maps supplied by the New York City Department of Environmental Protection. The soil map was rasterized from the vector DLG file. The land-use map was obtained from the Natural Resources Conservation Service. These base maps were adapted by Frankenberger (1996) to fit grid dimensions of 10 m by 10 m. Soil parameters were obtained from 'A GIS-Based Variable Source Area Model' developed by Frankenberger (1996). Daily soil moisture distribution maps generated by Frankenberger's model were used as the initial soil moisture

Table 1. Summary of model calibration and its parameters

Storm event	Total rainfall (mm)	Manning's n Stream	Forest	Grass /Alfalfa	Corn	Farm -stead	Hydraulic conductivity (m/day) high SMA*	low SMA	Initial soil moisture adjustment ratio stony	silt loam	Total runoff (mm) Obs.	Pre.	Peak discharge (m^3/sec) Obs.	Pre.
7/02/94	24.02	0.03	0.15	0.14	0.17.	0.09	1.20	0.80	1.066	1.072	1.72	1.64	0.234	0.235
7/22/94	24.76	0.02	0.26	0.20	0.23	0.12	2.00	0.80	0.520	0.560	1.17	1.00	0.236	0.230
8/18/94	22.62	0.04	0.20	0.14	0.17	0.09	1.20	0.80	0.610	0.690	5.99	5.54	0.276	0.267
Mean		0.03	0.20	0.16	0.19	0.10	1.47	0.80						

* SMA : soil moisture area

Table 2. Summary of model verification

Storm event	Total rainfall (mm)	Initial soil moisture adjustment ratio stony	silt loam	Total runoff (mm) observed	predicted	Peak discharge (m^3/sec) observed	predicted	Nash-Sutcliffe efficiency R^2
8/14/94	25.80	1.180	1.230	2.30	1.94	0.209	0.201	0.754
8/17/94	17.68	1.071	1.076	2.04	1.83	0.172	0.186	0.742
8/21/94	14.64	1.066	1.072	3.18	2.90	0.256	0.242	0.653

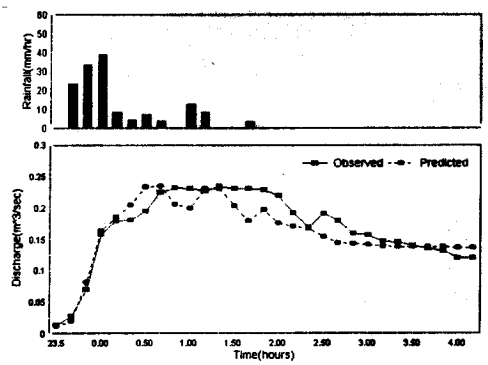

Figure 3. Comparison of predicted and observed stream flow (July 2, 1994 at Crowe Road watershed)

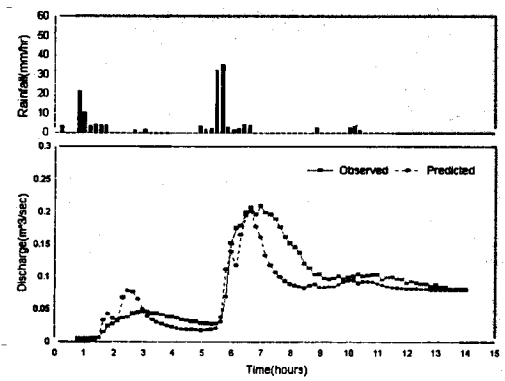

Figure 4. Comparison of predicted and observed stream flow (August 14, 1994 at Crowe Road watershed)

conditions for the selected storm events. These maps form 151 rows by 174 columns ASCII-formatted map data.

3.3 Comparing predicted and observed streamflow at the watershed outlet

Three storm events (July 2, July 22, August 18) were used for model calibration. The first two events had dry initial soil moisture conditions, and the last event had wet initial conditions due to the previous day's rainfall. The previous day's soil moisture distribution maps from Frankenberger's model were originally chosen as the initial soil moisture conditions for the storm events. But it was adjusted for two main reasons. Firstly, the value of r^2 in her study was only 0.45 for the simulated moisture contents versus a moving average of measured soil moisture contents where the measured soil moisture content ranged from 0.25 m^3/m^3 to 0.45 m^3/m^3. Secondly, the simulated soil moisture distribution is the result of daily soil moisture routing which should be adjusted for the rainfall time within a day. To simplify the adjustment of initial soil moisture

conditions, the watershed's 11 soil types were categorized into 2 groups: stony and silt loam. A constant adjustment factor was applied to the simulated soil moisture contents in all grid elements. The factor ranged from 0.520 for stony soils during the July 22 storm to 1.072 for silt loam soils during the July 2 storm.

In the model calibration, the initial soil moisture distribution before the storm event proved to be the most sensitive parameter affecting stream flow at the watershed outlet. The second most sensitive parameter was Manning's roughness coefficients for overland areas and streams which affected the time and magnitude of the peak stream flow. As an example of the observed versus predicted stream flow at the watershed outlet, Figure 3 shows the July 2 storm. The predicted runoff agreed well with the observed values. Table 1 shows the calibrated parameters for all three storm events.

The model was verified using the calibrated parameters from Table 1 (except the soil moisture adjustment factors which differ for each storm-event/soil-group combination) to predict stream flows at the watershed outlet for three new storms (August 14, August 17, August 21). The adjustment factor for initial soil moisture ranged from 1.066 for stony soil during the August 21 storm, to 1.230 for silt loam soil during the August 14 storm. The predicted outlet stream flows for the three storms were compared with observed values. As an example of the predicted versus observed stream flow, Figure 4 shows the August 14 storm. A summary of model verification is given in Table 2. The average Nash-Sutcliffe efficiency R^2 (Nash and Sutcliffe, 1970) for the model was 0.72. The total runoff was underestimated for three events. This error may be caused by the simplification of subsurface flow. Preferential flow through macro-pores in the soil can contribute to stream flow as a subsurface lateral flow. Other sources of error may arise from the uncertainty of initial soil moisture condition and lumping parameters within each 10 m by 10 m grid element.

3.4 Temporal variation and spatial distribution of saturation overland flow

Knowing only the stream flow at the watershed

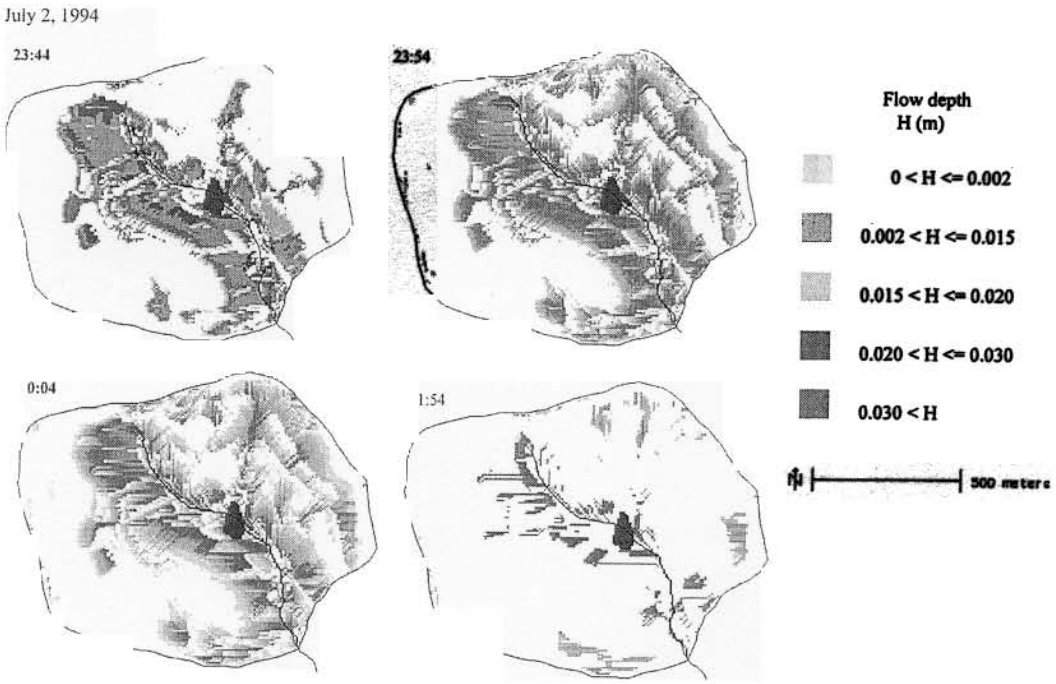

Figure 5. Temporal variation and spatial distribution of overland flow depth (July 2, 1994 at Crowe Road Watershed)

outlet, we cannot determine where the overland flow originated and how much water each source area contributed. GIS can provide this information which is important for investigating the loss of soil due to erosion and the transport of non-point source pollutants.

Figure 5 shows the predicted temporal and spatial distribution of saturated overland flow depths for the July 2 storm. After the storm started at the time of 23:24 hr, the overland flow areas initially occurred around the areas of the main stream. These areas have mild slopes and higher initial soil moisture content than other areas. The source area for overland flow increased from the start of rainfall to the time of 23:54 hr and decreased gradually after that time. But the peak flow reached at the time of 0:40 hr as in Figure 3. This shows that the overland/subsurface flows delayed the transport of water to the watershed outlet causing a lag time.

From the spatial distribution of soil moisture content before and after the same storm event, it is apparent that there was a soil moisture change especially in Vl (Vly channery silt loam) soils.

4. CONCLUSIONS

Grid-based storm runoff model was developed. This model generates the flow depth, discharge and soil moisture of subsurface flow and saturated overland flow on a variable source area with shallow soil depths. The model uses regular gridded ASCII-formatted data from GRASS to predict the temporal variation and spatial distribution of saturation overland flow areas.

The model was tested on a small watershed located in the Northern Catskill region of New York State with 10 m by 10 m grid dimensions. For model calibration and verification, the observed stream flows measured at watershed outlet were compared with values predicted by the model. The spatial distributions of saturated overland flow areas for several storm events were successfully modeled and displayed with GRASS. The calculated overland flow areas coincided with the areas which had high initial soil moisture contents. Temporal variation of those areas showed that the overland/subsurface flows attenuate and causes lag in the stream flows. This model can be used on other raster-based GIS if ASCII-formatted grid data are available.

REFERENCES

Allen, S. J., Digital hydrologic modeling methods for water resources engineering with application to the Broad Brook Watershed, Ph.D. thesis, University of Connecticut, 1987.

Brakensiek, D. L., Kinematic flood routing, Trans. ASAE, 10, 340-343, 1967.

Dunne, T. and Black, R. D., Partial area contributions to storm runoff in a small New England watershed, Water Resour. Res., 6, 1296-1311, 1970.

Famiglietti, J. S., Aggregation and scaling of spatially-variable hydrological process: Local catchment-scale and macroscale models of water and energy balance, Ph.D. thesis, University of Maryland, College Park, 1992.

Frankenberger, J. R., Identification of critical runoff generating areas using a variable source area model. Ph.D. thesis, Cornell University, Ithaca NY, 1996.

Kirkby, M. J., Hillslope Hydrology, John Wiley & Sons, 1978.

Moore, I. D., and G. J. Burch, Sediment transport capacity of sheet and rill flow: Application of unit stream power theory, Water Resour. Res., 22, 1350-1360, 1986.

Moore, I. D., and G. R. Foster, Hydraulics and overland flow, in Process Studies in Hillslope Hydrology, edited by M. G. Anderson and T. P. Burt, pp.215-254, John Wiley, New York, 1990.

Moore, I. D., and R. B. Grayson, Terrain-based catchment partitioning and runoff prediction using vector elevation data, Water Resour. Res., 27, 1177-1191, 1991.

Nash, J. E. and J. V. Sutcliffe, River flow forecasting through conceptual models, Part I - A discussion of principles, J. of Hydrol., 10, 283-290, 1970.

Stuebe, M. M., and D. M. Johnston, Runoff volume estimation using GIS techniques, Water Resour. Bull. 26(4), 611-620, 1990.

Savabi, M. R., D. C. Flanagan, B. A. Engel, M. A. Nearing, and B. Hebel, Application of WEPP and GIS to predict storm runoff: Proceedings of the international symposium on water quality modeling, pp. 348-357, Orlando FL, 1995.

Takasao, T., and M. Shiiba, Incorporation of the effect of concentration of flow into the kinematic wave equations and its application to runoff system lumping, J. Hydrol., 102, 301-322, 1988.

Tischendorf, W. G., Tracing stormflow to varying source area in small forested watershed in the southeastern piedmont, Ph.D. thesis, Univ. Georgia, Athens, 1969.

US Army CERL, GRASS 4.1 User's Manual,

Construction Engineering Research Laboratory, Champaign, IL, 1993.

Zollweg, J. A., Effective use of Geographic Information Systems for rainfall-runoff modeling, Ph.D. thesis, Cornell University, 1994.